Inorg. Chem. **2007**, *46*, 1694–1703

Triferrocenes Built on a C_3-Symmetric Ligand Platform: Entry to Redox-Active *pseudo*-Triphenylenes via Chelation-Driven Stereoselection of Triple Schiff Bases

Young-Kwan Lim, Scott Wallace, John C. Bollinger, Xufang Chen, and Dongwhan Lee*

Department of Chemistry, Indiana University, 800 East Kirkwood Avenue, Bloomington, Indiana 47405

Received October 23, 2006

An expedient tandem deprotonation–trapping protocol was employed to prepare a tris(difluoroboronyl) complex of a triferrocenyl ligand that is geometrically analogous to substituted triphenylenes. A triple Schiff base condensation reaction between 1,3,5-triformylphloroglucinol and aminoferrocene afforded the tris(*N*-salicylideneamine) adducts **5a** + **5b** in ca. 1:1 ratio. The keto–enamine tautomeric core of this isomeric mixture could be converted to a common enolate–imine intermediate. Subsequent trapping with $BF_3 \cdot Et_2O$ cleanly afforded the tris(difluoroboronyl) adduct **6** in essentially quantitative yield. The electronic and structural properties of this new class of ferrocene compounds were investigated using various methods including UV–vis, cyclic voltammetry (CV), differential pulse voltammetry (DPV), and X-ray crystallography. In CH_2Cl_2–CH_3CN, **6** displayed a reversible three-electron oxidation process at $E_{1/2}^{ox} = +210$ mV (vs Fc/Fc^+). Despite the sharing of a common [π,π]/[n,π]-conjugated core, no significant electronic communication was observed among the three ferrocenyl units in **6** under either CV or DPV conditions. On the other hand, the broad oxidation wave of **5a** + **5b** at $E_{1/2}^{ox} = +60$ mV in CH_2Cl_2–CH_3CN was comprised of at least two major components at +20 and +90 mV, which collapsed to become a single peak in DMF electrolyte, despite that the ratios between the two isomers **5a**,**b** remained essentially invariant to the change in solvent.

Introduction

Transition metal complexes displaying multielectron redox chemistry have attracted much attention due to their potential applications in molecular materials for catalysis, charge transport, and electron storage. Compounds containing multiple ferrocene (Fc) units represent one such example,[1−5] in which the well-defined redox chemistry of Fc serves as a powerful electrochemical probe to investigate ground-state electronic coupling through space or through bonds. Detailed understanding of such processes in small molecules would provide an important foundation for designing and constructing electroactive materials[6] in which macromolecular scaffolds can systematically control *cross communication* between adjacent redox-active sites to provide well-defined conduits for charge transport.[5−9]

In contrast to extensive synthetic efforts devoted to one-dimensional (1-D) systems incorporating multiple Fc units within linearly π-conjugated manifolds **(A)**,[1−5,10,11] parallel progress in two-dimensional (2-D) systems (**B**) has produced only a handful of structurally characterized oligoferrocene compounds.[12,13] As shown in Figure 1, planar conjugated

* To whom correspondence should be addressed. E-mail: dongwhan@indiana.edu.

(1) (a) Togni, A., Hayashi, T., Eds. *Ferrocenes*; VCH: Weinheim, Germany, 1995. (b) *J. Organomet. Chem*. **2001**, *637*−*639*, a special issue on ferrocene chemistry.
(2) Barlow, S.; O'Hare, D. *Chem. Rev.* **1997**, *97*, 637−669.
(3) Astruc, D. *Acc. Chem. Res.* **1997**, *30*, 383−391.
(4) Wagner, M. *Angew. Chem., Int. Ed.* **2006**, *45*, 5916−5918.
(5) Manners, I. *Synthetic Metal-Containing Polymers*; Wiley-VCH: Weinheim, Germany, 2004.
(6) Pickup, P. G. *J. Mater. Chem.* **1999**, *9*, 1641−1653.
(7) Wolf, M. O. *Adv. Mater.* **2001**, *13*, 545−553.
(8) Weder, C. *Chem. Commun.* **2005**, 5378−5389.
(9) Holliday, B. J.; Swager, T. M. *Chem. Commun.* **2005**, 23−36.
(10) For examples of oligoethynyl-bridged diferrocenes, see the following: (a) Rosenblum, M.; Brawn, N.; Papenmeier, J.; Applebaum, M. *J. Organomet. Chem.* **1966**, *6*, 173−180. (b) Levanda, C.; Bechgaard, K.; Cowan, D. O. *J. Org. Chem.* **1976**, *41*, 2700−2704. (c) Yuan, Z.; Stringer, G.; Jobe, I. R.; Kreller, D.; Scott, K.; Koch, L.; Taylor, N. J.; Marder, T. B. *J. Organomet. Chem.* **1993**, *452*, 115−120. (d) Adams, R. D.; Qu, B.; Smith, M. D. *Organometallics* **2002**, *21*, 3867−3872. (e) Xu, G.-L.; Xi, B.; Updegraff, J. B.; Protasiewicz, J. D.; Ren, T. *Organometallics* **2006**, *25*, 5213−5215.

10.1021/ic062029v CCC: $37.00
Published on Web 01/23/2007

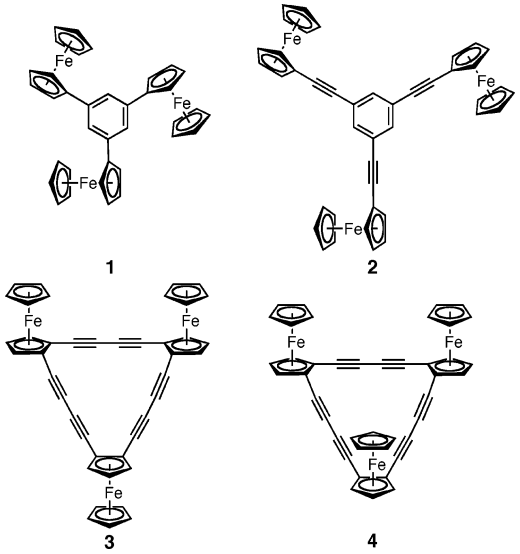

Figure 1. Chemical structures of representative triferrocenes.[14,16,17]

triferrocene compounds could be constructed either (a) by using C_3-symmetric π-conjugated cores (**1**[14,15] and **2**,[16] Figure 1) or (b) by directly linking cyclopentadienyl groups to define a rigid cyclic array (**3** and **4**,[17,18] Figure 1). In these trimetallic constructs, electronic coupling between individual redox-active sites strongly depends on the nature of the C_3-symmetric "bridges". For example, **1**[14d] and **2**[16] show three-electron redox chemistry at a single oxidation potential,[19] whereas **3** displays three sequential one-electron oxidation processes indicative of the formation of detectable mixed-valent intermediates.[17,20] Intriguingly, compound **4**, being chemically equivalent to but stereochemically distinctive from **3**, undergoes two reversible redox processes involving one and two electrons, respectively.[17] Studies of such conformationally well-defined triferrocenes should sharpen our understanding of charge delocalization in 2-D conjugation in general.

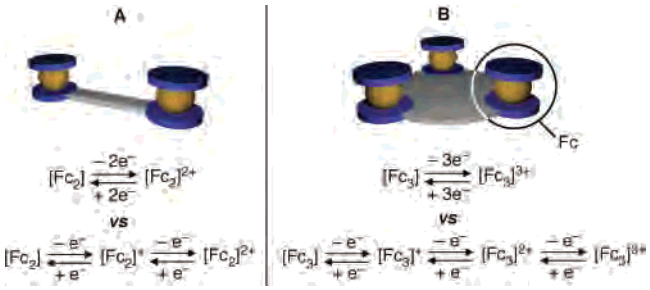

We have recently shown that an efficient two-step synthetic protocol can facilitate access to planar-rigid C_3-symmetric molecules that are geometrically analogous to 2,6,10-trisubstituted triphenylenes.[21] Notably, the modular nature of this simple and high-yielding synthetic sequence was ideal for installing multiple functionalities in a spatially well-defined manner, prompting us to construct redox-active *pseudo*-triphenylenes having three ferrocenyl fragments disposed in C_3-symmetric fashion. In addition to expanding the family of oligoferrocenes built on planar rigid scaffolds,[14−18] convincing structural evidence for the elusive *pseudo* C_s-isomeric form of tris(*N*-salicylideneamine)[21−24] was obtained by X-ray crystallography. Notably, the three ferrocenyl units in the tris(*N*-salicylideneamine) compounds **5a** + **5b** and their tris(difluoroboronyl) adduct **6** displayed markedly different electrochemical behavior. The design, synthesis, and characterization of these compounds are described in this paper.

(11) For examples of heteroatom-bridged diferrocenes displaying strong electronic communication, see the following: (a) Jäkle, F.; Rulkens, R.; Zech, G.; Foucher, D. A.; Lough, A. J.; Manners, I. *Chem.*—Eur. J. **1998**, *4*, 2117−2128. (b) Venkatasubbaiah, K.; Zakharov, L. N.; Kassel, W. S.; Rheingold, A. L.; Jäkle, F. *Angew. Chem., Int. Ed.* **2005**, *44*, 5428−5433.

(12) Triferrocenes supported by C_3-symmetric phenylene-vinylene-based cores are known, but these "minidendrimers" have mainly been characterized spectroscopically: (a) Briel, O.; Fehn, A.; Beck, W. *J. Organomet. Chem.* **1999**, *578*, 247−251. (b) Peruga, A.; Mata, J. A.; Sainz, D.; Peris, E. *J. Organomet. Chem.* **2001**, *637*−*639*, 191−197. (c) Palomero, J.; Mata, J. A.; González, F.; Peris, E. *New J. Chem.* **2002**, *26*, 291−297. (d) König, B.; Zieg, H.; Bubenitschek, P.; Jones, P. G. *Chem. Ber.* **1994**, *127*, 1811−1813.

(13) For a recent example of a dendritic hexaferrocene compound built on a hexakis(4-phenyl)benzene platform, see the following: Chebny, V. J.; Dhar, D.; Lindeman, S. V.; Rathore, R., *Org. Lett.* **2006**, *8*, 5041−5044.

(14) (a) Schlögl, K.; Soukup, H. *Tetrahedron Lett.* **1967**, *8*, 1181−1184. (b) Rosenblum, M.; Brawn, N.; King, S. J.; King, B. *Tetrahedron Lett.* **1967**, *8*, 4421−4425. (c) Sasaki, Y.; Pittman, C. U., Jr. *J. Org. Chem.* **1973**, *38*, 3723−3726. (d) Iyoda, M.; Kondo, T.; Okabe, T.; Matsuyama, H.; Sasaki, S.; Kuwatani, Y. *Chem. Lett.* **1997**, 35−36. (e) Gupta, H. K.; Reginato, N.; Ogini, F. O.; Brydges, S.; McGlinchey, M. J. *Can. J. Chem.* **2002**, *80*, 1546−1554. (f) Stepnicka, P.; Cisarova, I.; Sedlacek, J.; Vohlidal, J.; Polasek, M. *Collect. Czech. Chem. Commun.* **1997**, *62*, 1577−1584.

(15) For 1,2,4-triferrocenylbenzene, see the following: (a) Mathur, P.; Singh, A. K.; Singh, V. K.; Singh, P.; Rahul, R.; Mobin, S. M.; Thöne, C. *Organometallics* **2005**, *24*, 4793−4798. (b) Fiorentini, S.; Floris, B.; Galloni, P.; Grepioni, F.; Polito, M.; Tagliatesta, P. *Eur. J. Org. Chem.* **2006**, 1726−1732.

(16) Fink, H.; Long, N. J.; Martin, A. J.; Opromolla, G.; White, A. J. P.; Williams, D. J.; Zanello, P. *Organometallics* **1997**, *16*, 2646−2650.

(17) (a) Altmann, M.; Friedrich, J.; Beer, F.; Reuter, R.; Enkelmann, V.; Bunz, U. H. F. *J. Am. Chem. Soc.* **1997**, *119*, 1472−1473. (b) Bunz, U. H. F.; Roidl, G.; Altmann, M.; Enkelmann, V.; Shimizu, K. D. *J. Am. Chem. Soc.* **1999**, *121*, 10719−10726.

(18) The minimalist approach to this quest would be direct "fusion" of three ferrocenes. One such compound, bis(trindene)triiron, was reported but characterized by mass spectrometry only. See the following: Katz, T. J.; Slusarek, W. *J. Am. Chem. Soc.* **1980**, *102*, 1058−1063.

(19) It is noteworthy that the cyclic voltammograms of **1** confined within thin layers display two pairs of redox waves, which is quite different from the single three-electron redox process typically observed in conventional CV measurements.[14d] See the following: Li, Y.; Tsang, E. M. W.; Chan, A. Y. C.; Yu, H.-Z. *Electrochem. Commun.* **2006**, *8*, 951−955.

(20) Care should be exercised in using the ΔE values obtained in different matrix conditions, such as temperatures, solvents, and electrolytes, as a direct measure of the degree of electronic coupling. For examples of the dependence of ΔE on such experimental conditions, see the following: (a) LeSuer, R. J.; Geiger, W. E. *Angew. Chem., Int. Ed.* **2000**, *39*, 248−250. (b) Barriere, F.; Camire, N.; Geiger, W. E.; Mueller-Westerhoff, U. T.; Sanders, R. *J. Am. Chem. Soc.* **2002**, *124*, 7262−7263. (c) Barriere, F.; Geiger, W. E. *J. Am. Chem. Soc.* **2006**, *128*, 3980−3989.

(21) Riddle, J. A.; Lathrop, S. P.; Bollinger, J. C.; Lee, D. *J. Am. Chem. Soc.* **2006**, *128*, 10986−10987.

(22) (a) Chong, J. H.; Sauer, M.; Patrick, B. O.; MacLachlan, M. J. *Org. Lett.* **2003**, *5*, 3823−3826. (b) Sauer, M.; Yeung, C.; Chong, J. H.; Patrick, B. O.; MacLachlan, M. J. *J. Org. Chem.* **2006**, *71*, 775−788. (c) Yelamaggad, C. V.; Achalkumar, A. S.; Rao, D. S. S.; Prasad, S. K. *J. Am. Chem. Soc.* **2004**, *126*, 6506−6507.

(23) Riddle, J. A.; Bollinger, J. C.; Lee, D. *Angew. Chem., Int. Ed.* **2005**, *44*, 6689−6693.

(24) Jiang, X.; Bollinger, J. C.; Lee, D. *J. Am. Chem. Soc.* **2006**, *128*, 11732−11733.

Experimental Section

General Considerations. All reagents were obtained from commercial suppliers and used as received unless otherwise noted. Tetrahydrofuran was saturated with nitrogen and purified by passage through activated Al_2O_3 columns under nitrogen (Innovative Technology SPS 400).[25] The compounds 1,3,5-triformylphloroglucinol[22a] and *N*-(*o*-hydroxybenzylidene)ferroceneamine (**7**)[26] were prepared according to literature procedures. A modified procedure was used in the synthesis of aminoferrocene, which did not require isolation of air-sensitive and pyrophoric lithioferrocene[27] as the synthetic precursor to the key intermediate *N*-ferrocenyl phthalimide. All air-sensitive manipulations were carried out under nitrogen atmosphere by standard Schlenk-line techniques.

Aminoferrocene. To an anhydrous THF solution (150 mL) of ferrocene (10.0 g, 53.8 mmol) at 0 °C under nitrogen was added dropwise *tert*-BuLi (32.0 mL, 54 mmol, 1.7 M solution in pentane). The heterogeneous mixture was stirred at 0 °C for 15 min. An anhydrous THF solution (50 mL) of 1,2-diiodoethane (15.15 g, 53.75 mmol) was added by cannula, and the reaction mixture was warmed to room temperature. The reaction was quenched by treating with a saturated aqueous solution (100 mL) of $Na_2S_2O_3$ and extracted with EtOAc (100 mL × 3). The combined extracts were dried over anhydrous $MgSO_4$, filtered, and concentrated under reduced pressure to afford crude iodoferrocene (14.80 g, 45.96 mmol), which was mixed with phthalimide (10.15 g, 68.98 mmol) and Cu_2O (3.29 g, 23.0 mmol) in anhydrous pyridine (100 mL). The reaction mixture was heated at 130 °C for 24 h, cooled to room temperature, concentrated, and purified by column chromatography on SiO_2 (10:1 hexanes−EtOAc) to afford *N*-ferrocenyl phthalimide[27] as red crytals (7.48 g, 22.6 mmol, overall 42% yield in two steps). This compound was converted to aminoferrocene by hydrazinolysis in EtOH by following literature procedure.[27,28]

2,4,6-Tris(ferrocenylmethylene)cyclohexane-1,3,5-trione (5a + 5b). An EtOH (50 mL) solution of aminoferrocene (3.05 g, 15.2 mmol) and 1,3,5-triformylphloroglucinol (631 mg, 3.00 mmol) was heated at reflux for 24 h to afford a burgundy red suspension. The reaction mixture was cooled to room temperature and filtered to isolate **5a** + **5b** (2.25 g, 99%) as a red solid, which was washed with Et_2O and dried in vacuo. ^{1}H NMR (400 MHz, $CDCl_3$): δ 12.85 (d, J = 12.8 Hz), 12.73 (d, J = 12.8 Hz), 12.30 (d, J = 13.6 Hz), 12.20 (d, J = 12.8 Hz), 8.58 (d, J = 12.8 Hz), 8.57 (d, J = 13.2 Hz), 4.54 (bs), 4.52 (bs), 4.26 (s), 4.25 (s), 4.24 (s), 4.22 (s), 4.18 (s), 4.16 (s). FT-IR (KBr pellet, cm^{-1}): 3090, 1597, 1550, 1435. UV−vis (CH_2Cl_2, λ_{max}, nm (ϵ, M^{-1} cm^{-1})): 370 (49 000), 475 (sh, 15 600). HRMS (CI): calcd for $C_{39}H_{34}N_3Fe_3O_3$ ([M + H]$^+$), 760.0648; found, 760.0649.

1,3,5-Tris(difluoroboronyloxy)-2,4,6-tris[(ferrocenylimino)methyl]benzene (6). A BF_3·Et_2O (20 mL) solution of **5a** + **5b** (2.50 g, 3.29 mmol) was cooled to 0 °C under nitrogen. A portion of lithium diisopropylamide (18 mL, 2.0 M in heptane/THF/ethylbenzene) was added dropwise over a period of 10 min, and the reaction mixture was warmed to room temperature and stirred for 24 h. The reaction was cooled to 0 °C and quenched by adding ice (20 g). A dark purple solid was isolated by filtration, washed with water, EtOH, and Et_2O, and dried in vacuo to afford **6** (3.05 g, 99%). ^{1}H NMR (400 MHz, $CDCl_3$): δ 9.02 (s, 3H), 4.91 (s, 6H), 4.47 (s, 6H), 4.35 (s, 15H). ^{11}B NMR (128.4 MHz, $CDCl_3$, externally referenced to BF_3·Et_2O at δ = 0.00 ppm): δ 0.24. ^{19}F NMR (282.3 MHz, $CDCl_3$, externally referenced to CF_3CO_2H at δ = −78.5 ppm): δ −100.5. FT-IR (KBr pellet, cm^{-1}): 3210, 2362, 2261, 1613, 1564. UV−vis (CH_2Cl_2, λ_{max}, nm (ϵ, M^{-1} cm^{-1})): 360 (33 500), 560 (6350). HRMS (CI): calcd for $C_{39}H_{30}N_3B_3F_6Fe_3O_3$ ([M + H]$^+$), 904.0597; found, 904.0524.

2-((Difluoroboronyl)oxy)-1-[(ferrocenylimino)methyl]benzene (8). This compound was prepared from **7** (0.46 g, 1.5 mmol), lithium diisopropylamide (1.5 mL, 2.0 M in heptane/THF/ethylbenzene), and BF_3·Et_2O (10 mL) in a manner similar to that described for **6**. The product was isolated as a dark purple solid (0.46 g, 87%). ^{1}H NMR (400 MHz, $CDCl_3$): δ 8.58 (s, 1H), 7.62 (t, J = 7.6 Hz, 1H), 7.42 (d, J = 7.6 Hz, 1H), 7.10 (d, J = 8.4 Hz, 1H), 6.99 (t, J = 7.6 Hz, 1H), 4.94 (s, 2H), 4.49 (s, 2H), 4.38 (s, 5H). ^{11}B NMR (128.4 MHz, $CDCl_3$, externally referenced to BF_3·Et_2O at δ = 0.00 ppm): δ 0.45 (t, J = 14.70 Hz). ^{19}F NMR (282.3 MHz, $CDCl_3$, externally referenced to CF_3CO_2H at δ = −78.5 ppm): δ −135.4. FT-IR (KBr pellet, cm^{-1}): 3210, 3100, 2362, 2261, 1614, 1557, 1484. UV−vis (CH_2Cl_2, λ_{max}, nm (ϵ, M^{-1} cm^{-1})): 315 (10 400), 370 (5940), 545 (1510). HRMS (CI): calcd for $C_{17}H_{14}NBF_2FeO$ ([M]$^+$), 353.0486; found, 353.0471.

X-ray Crystallographic Studies. Intensity data were collected on a Bruker diffractometer equipped with a SMART 6000 CCD detector. A typical single crystal was selected from the bulk sample and affixed to the tip of a glass fiber with the use of silicone grease, and the mounted sample was transferred to the goniostat and cooled to −144 °C (for **6**) or −155 °C (for **8**) for characterization and data collection. Frames were measured for 5 s each with a frame width of 0.3 degrees in ω. A face-indexed absorption correction was applied, and data were corrected for instrumental effects, interframe scaling differences, and other systematic errors via the SADABS program.[29] Equivalent reflections were averaged. The structure was solved by direct methods and completed by Fourier techniques using the SHELXTL software package.[30] For **6**, all hydrogen atoms were placed in idealized positions and refined according to a riding model. For **8**, all hydrogen atoms were located in a difference electron density map and refined as isotropic contributors in the final cycles of least squares. All non-hydrogen atoms were refined anisotropically unless otherwise noted. One of the cyclopentadienyl (Cp) groups of **6** was disordered over two positions with partial occupancies of 0.51 and 0.49. The structure of **6** also contains lattice solvent molecules nitromethane and dichloroethane at two distinct positions. One solvent position contains an ordered nitromethane molecule, but the other contains two distinct nitromethane orientations and one dichloromethane, all overlapping, in a ratio close to 2:1:1. Geometric and thermal parameter restraints were applied to these closely overlapping disorder components, and they were refined with isotropic thermal parameters. The structure of **5a** + **5b** was not fully refined owing to disorder in the molecular core, ferrocenyl fragments, and solvent molecules. This compound crystallizes in triclinic space group $P\bar{1}$ with a = 10.537(4) Å, b = 17.078(6) Å, c = 21.364(7) Å, α = 79.169(8)°, β = 89.467(8)°, γ = 73.791(7)°, and Z = 4. Crystallographic information is provided in Table 1.

(25) Pangborn, A. B.; Giardello, M. A.; Grubbs, R. H.; Rosen, R. K.; Timmers, F. J. *Organometallics* **1996**, *15*, 1518−1520.
(26) Bracci, M.; Ercolani, C.; Floris, B.; Bassetti, M.; Chiesi-Villa, A.; Guastini, C. *J. Chem. Soc., Dalton Trans.* **1990**, 1357−1363.
(27) Bildstein, B.; Malaun, M.; Kopacka, H.; Wurst, K.; Mitterböck, M.; Ongania, K.-H.; Opromolla, G.; Zanello, P. *Organometallics* **1999**, *18*, 4325−4336.
(28) Heinze, K.; Schlenker, M. *Eur. J. Inorg. Chem.* **2004**, 2974−2988.
(29) Sheldrick, G. M. *SADABS 2006/1: Bruker Nonius area detector scaling and absorption correction*; University of Göttingen: Göttingen, Germany, 2006.
(30) *SHELXTL v6.12*; Bruker Analytical X-Ray Solutions: Madison, WI, 2001.

Table 1. Summary of X-ray Crystallographic Data

param	**6**·1.75CH_3NO_2·0.25CH_2Cl_2	**8**
formula	$C_{41}H_{35.75}B_3Cl_{0.50}F_6Fe_3N_{4.75}O_{6.50}$	$C_{17}H_{14}BF_2FeNO$
fw	1030.70	352.95
space group	$P\bar{1}$	$P2_1/n$
a, Å	10.447(3)	6.229(3)
b, Å	10.885(2)	14.553(8)
c, Å	18.647(4)	15.613(8)
α, deg	93.915(13)	
β, deg	99.125(11)	94.481(15)
γ, deg	106.223(16)	
V, Å^3	1996.0(7)	1411.0(13)
Z	2	4
ρ_{calcd}, g/cm^3	1.715	1.661
T, °C	−144	−155
μ(Mo Kα), mm^{-1}	1.196	1.093
θ limits, deg	1.96−27.50	3.83−37.97
tot. no. of data	45 630	19 024
no. of unique data	9180	4109
no. of params	646	264
R (%)[a]	3.60	3.10
wR^2 (%)[b]	9.83	7.75
Max, min peaks, e/Å^3	0.907, −0.636	0.511, −0.302

[a] $R = \sum||F_o| - |F_c||/\sum|F_o|$. [b] $wR^2 = \{\sum[w(F_o^2 - F_c^2)^2]/\sum[w(F_o^2)^2]\}^{1/2}$.

Physical Measurements. ^{1}H NMR and ^{13}C NMR spectra were recorded on a 400 MHz Varian Inova NMR spectrometer or a 300 MHz Varian Gemini 2000 NMR spectrometer. Chemical shifts were reported versus tetramethylsilane and referenced to the residual solvent peaks. High-resolution chemical ionization (CI) and electrospray ionization (ESI) mass spectra were obtained on a Thermo Electron Corp. MAT 95XP-Trap using CH_4 as CI reagent. FT-IR spectra were recorded on a Nicolet 510P FT-IR spectrometer with EZ OMNIC ESP software. UV−vis spectra were recorded on a Perkin-Elmer Lambda 19 UV/vis/NIR spectrometer.

Electrochemistry. Electrochemical studies were carried out under nitrogen with an Autolab model PGSTAT30 potentiostat (Eco Chemie). A three-electrode configuration consisting of a platinum button as the working electrode, a $Ag/AgNO_3$ (0.01 M in CH_3CN with 0.1 M (n-Bu_4N)(PF_6)) reference electrode, and a platinum coil counter electrode was used. The supporting electrolyte was 0.1 M (*n*-Bu_4N)(PF_6) either in CH_2Cl_2−CH_3CN (1:1, v/v) or in DMF. All electrochemical potentials are reported to the Cp_2Fe/Cp_2Fe^+ redox couple.

Results

Synthesis and Structural Characterization. Synthetic routes to triferrocenes **5a** + **5b** and **6** are outlined in Scheme 1. An efficient large-scale synthesis of aminoferrocene,[26−28,31,32] a key building block in our modular synthesis, was facilitated by adapting conditions developed for structurally more elaborate Fc derivatives.[33] Specifically, lithioferrocene, generated in situ from the reaction between Fc and ^{t}BuLi at 0 °C, was reacted with diiodoethane to afford iodoferrocene, which was converted without further purification to *N*-ferrocenyl phthalimide in overall 42% yield. Simple hydrazinolysis of this material under standard conditions[27,28] furnished gram quantities of aminoferrocene. In this modified scheme, no laborious purification of air-sensitive lithioferrocene intermediate was required.

Scheme 1

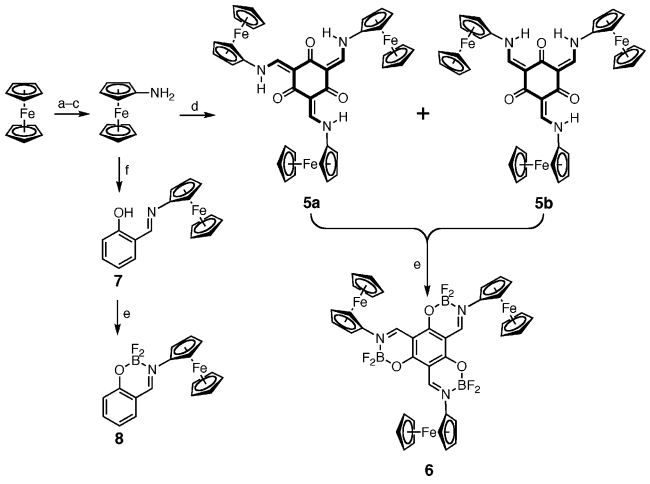

[a] ^{t}BuLi, ICH_2CH_2I, THF, 0 °C. [b] phthalimide, Cu_2O, pyridine, Δ. [c] H_2NNH_2·H_2O, EtOH, r.t. [d] 1,3,5-triformylphloroglucinol, EtOH, Δ. [e] BF_3·Et_2O, LDA. [f] salicylaldehyde, EtOH, Δ

The condensation reaction between 1,3,5-triformylphloroglucinol and 3 equiv of aminoferrocene proceeded cleanly in refluxing EtOH to furnish the triple Schiff base product in essentially quantitative yield (>99%) but as a mixture of two geometric isomers **5a** and **5b** (Scheme 1). The ^{1}H NMR spectrum of this material in $CDCl_3$ at 25 °C displayed complicated splitting patterns associated with the enamine N−H protons (12.21−12.87 ppm) and vinyl C−H protons (8.43−8.59 ppm) (Figure 2), the assignment of which was aided by 2D TOCSY spectroscopy (Figure S1). As shown in Figure 2, the three N−H protons and three C−H protons of the *pseudo*-C_3-symmetric **5a** furnish one unique set of doublets (J = 12.8 Hz) (blue, Figure 2) that are coupled through the C−N single bonds. On the other hand, **5b**, lacking this local rotational symmetry, provides unique magnetic environment for each of the three enamine fragments. As a result, three N−H doublets and three C−H doublets were observed instead (red, Figure 2). In $CDCl_3$ at 298 K the ratio between **5a** and **5b**, as quantified by peak integration, was approximately 1:0.83. Similar results were obtained in hydrogen-bonding solvent DMF-d_7, in which **5a** and **5b** coexist in ca. 1:1 ratio.

The stereoisomerism associated with the tris(*N*-salicylideneamine) core of **5a** + **5b** was subsequently confirmed by crystallographic chemical analysis. A dark red single crystal was obtained by diffusion of pentanes into a saturated 1,2-dichloroethane solution of this material. As shown in Figure 3a, two chemically equivalent but conformationally distinct molecules constitute the asymmetric unit, in which efficient packing in the solid state is aided by significant van der Waals contacts between two interlocked conformers, "all-up" (**C**) and "two-up, one-down" (**D**),[14e,f] differing in the ferrocenyl groups' disposition relative the planar core. The tris(*N*-salicylideneamine) core of the conformer **C** was disordered over two positions with a ratio of ca. 0.4:0.6, each corresponding to the *pseudo*-C_3-symmetric **5a** (Figure 3b). For the conformer **D**, the molecular core could be best

(31) Herberhold, M.; Ellinger, M.; Kremnitz, W. *J. Organomet. Chem.* **1983**, *241*, 227−240.
(32) Butler, D. C. D.; Richards, C. J. *Organometallics* **2002**, *21*, 5433−5436.
(33) Anderson, C. E.; Donde, Y.; Douglas, C. J.; Overman, L. E. *J. Org. Chem.* **2005**, *70*, 648−657.

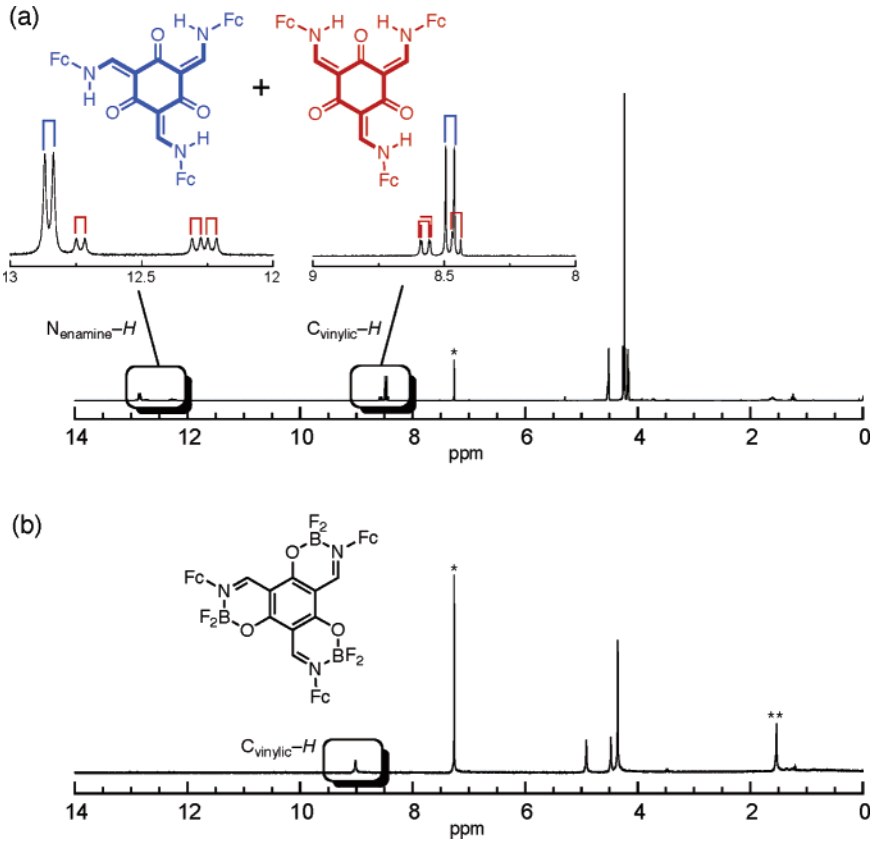

Figure 2. (a) ^{1}H NMR spectrum (400 MHz, 298 K) of **5a** + **5b** in $CDCl_3$. The isomer **5a** having local C_3-symmetry contributes one set of $N_{enamine}$−H and $C_{vinylic}$−H doublets that are coupled to each other (blue), whereas distinctive magnetic environments in less symmetric **5b** result in three pairs of $N_{enamine}$−H doublets and $C_{vinylic}$−H doublets (red) of essentially equal intensities. (b) ^{1}H NMR spectrum (400 MHz, 298 K) of **6** in $CDCl_3$. Residual solvent peaks are marked as ∗ (for $CHCl_3$) and ∗∗ (for H_2O).

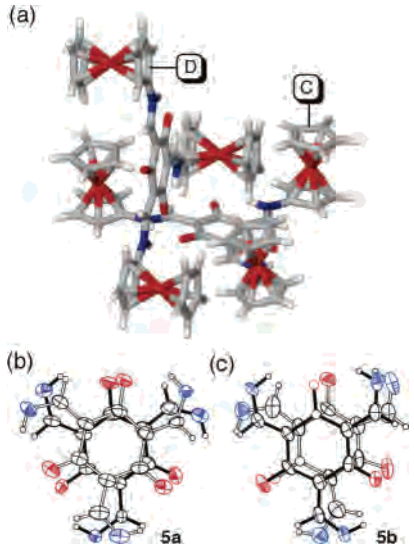

Figure 3. (a) Capped-stick representation of the solid-state structure of **5a** + **5b** showing the closely packed "all-up" (**C**) and "two-up, one-down" (**D**) conformers constituting the asymmetric unit. For clarity, only one disordered component of the model used in structure refinement is shown for each conformer. (b) Disordered core structure of **C** modeled as two overlaid tris(*N*-salicylideneamine) units of local C_{3h} symmetry. (c) Disordered core structure of **D** modeled as two overlaid tris(*N*-salicylideneamine) units of local C_s symmetry. For (b) and (c), ferrocenyl fragments have been omitted for clarity. N is blue, and O is red.

modeled as a superimposition of two **5b** components with a ratio of ca. 0.8:0.2 (Figure 3c). The Fe···Fe distances in **C** are dispersed in the range between 10.69 and 11.44 Å. Comparable metric parameters of 10.70−11.47 Å were obtained for **D**.

Although full structure refinement with diffraction data was hampered by this core disorder as well as the disorder of multiple ferrocenyl groups and lattice solvent molecules,[34] the chemical connectivity of **5a** + **5b** unequivocally established the presence of the two isomeric tris(*N*-salicylideneamine) cores, which has previously been deduced only from solution spectroscopic studies of related compounds.[21,22]

The stereochemical inhomogeneity associated with the tris(*N*-salicylideneamine) core of **5a** + **5b** could readily be eliminated by one-pot synthetic protocol involving deprotonation and in situ trapping with BF_3·Et_2O (Scheme 1). Analytically pure tris(difluoroboronyl) adduct **6** could be obtained in essentially quantitative yield following simple filtration and washing. A single sharp ^{1}H resonance (9.02 ppm, 3H) of the vinyl protons (Figure 2b) along with single ^{19}F (−100.5 ppm vs CF_3CO_2H with $\delta = -78.5$ ppm) and ^{11}B (0.24 ppm vs BF_3·Et_2O with $\delta = 0.00$ ppm) resonances

(34) In the structure refinement, the chemical symmetry of the molecules in the model was used to create extensive geometric restraints. As such, the results do not meet the publication criteria that are conventionally applied to small-molecule structures. Although the structural disorder is too pervasive to draw reliable conclusions about geometric details, the model described in Figure 3 explains the observed electron density comparatively well. This model is also consistent with the coexistence of **5a** and **5b** in ca 1:1 ratio, which was determined by ^{1}H NMR spectroscopy of solution samples.

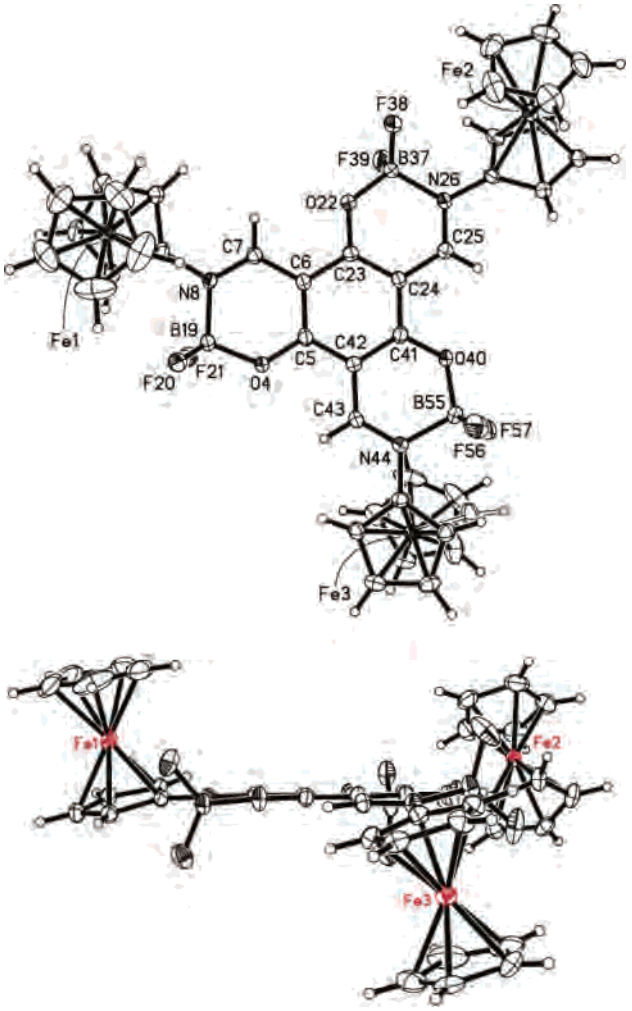

Figure 4. ORTEP diagram of **6** with thermal ellipsoids at 50% probability: top, top view; bottom, side view. The cyclopentadienyl ring attached to Fe(3) is disordered over two positions, for which only one model is shown for clarity.

indicated a highly symmetric core structure of **6**, which was subsequently confirmed by X-ray crystallography.

As shown in Figure 4, the three ferrocenyl groups of **6** are appended to a C_3-symmetric ring-fused $\{C_6O_3B_3(CN)_3\}$ core fragment which is geometrically analogous to triphenylene. The average deviation of the 18 atoms of $\{C_6O_3B_3(CN)_3\}$ from the idealized plane is 0.078(3) Å with maximum deviation of 0.228(3) Å for B(37). The sums of the internal angles of each of the three peripheral six-membered rings are 717.0, 717.7, and 719.3°. Similarly to **D** (Figure 3), the ferrocenyl groups of **6** adopt "two-up, one-down"[14e,f] conformation with dihedral angles of 16.6, 37.4, and 19.5° between the idealized $\{C_6O_3B_3(CN)_3\}$ plane and the peripheral cyclopentadienyl rings directly appended to it. Such small deviations from coplanarity might be due to extended π-conjugation that can potentially serve as pathways for electronic coupling. It should be noted, however, that the highly simplified cyclopentadienyl splitting patterns observed in the solution ^{1}H NMR spectrum of **6** (Figure 2b) implicate low-energy barrier C−N bond rotations, which would provide a population-averaged single environment on the NMR time scale. In the solid state, all three ferrocenyl groups display quasi-eclipsed conformation of the cyclopentadienyl rings. The Fe···Fe separations of 11.121, 11.488, and 11.550 Å are significantly narrowly dispersed compared with those in **5a** + **5b**, which apparently reflect the structural rigidity imposed by coordination of the $\{BF_2\}^+$ groups. The C−C bond distances of 1.406(3)−1.417(3) Å for the central six-membered central ring, C−O distances of 1.314(3)−1.318(3) Å, and C−N distances of 1.302(3)−1.307(3) Å are all consistent with the enol−imine, rather than the keto−enamine,[21−24,35] tautomer description of the tris(*N*-salicylideneamine) core of **6** (Table 2).

Table 2. Selected Bond Lengths (Å) and Angles (deg) for **6** and **8**[a]

		6	
O4−C5	1.310(3)	C42−C43	1.416(3)
O22−C23	1.318(3)	C6−C23	1.412(3)
O40−C41	1.314(3)	C23−C24	1.406(3)
C7−N8	1.302(3)	C24−C41	1.415(3)
C6−C7	1.417(3)	C41−C42	1.406(3)
C25−N26	1.307(3)	C5−C42	1.417(3)
C24−C25	1.418(3)	C5−C6	1.408(3)
C43−N44	1.304(3)		
N8−C7−C6	122.4(2)	C41−O40−B55	125.1(2)
C7−N8−B19	121.09(19)	O40−C41−C42	120.5(2)
O4−B19−N8	109.95(19)	C41−C42−C43	119.7(2)
C5−O4−B19	125.44(19)	N26−C25−C24	122.0(2)
O4−C5−C6	120.4(2)	C25−N26−B37	121.13(19)
C5−C6−C7	120.0(2)	O22−B37−N26	109.43(19)
N44−C43−C42	122.3(2)	C23−O22−B37	124.69(19)
C43−N44−B55	120.4(2)	O22−C23−C24	120.4(2)
O40−B55−N44	108.98(19)	C23−C24−C25	120.0(2)
		8	
C19−O20	1.3392(19)	C16−C17	1.400(2)
O20−B21	1.446(2)	C17−C18	1.386(2)
N12−B21	1.586(2)	C18−C19	1.394(2)
N12−C13	1.299(2)	C14−C19	1.409(2)
C13−C14	1.430(2)	C13−C14	1.430(2)
C14−C15	1.407(2)	N12−C13	1.299(2)
C15−C16	1.378(2)		
N12−C13−C14	121.91(14)	C19−O20−B21	123.10(12)
C13−N12−B21	120.74(13)	O20−C19−C14	120.66(14)
O20−B21−N12	110.52(12)	C19−C14−C13	119.18(14)

[a] Numbers in parentheses are estimated standard deviations of the last significant figures.

Compound **7**, which is a monoferrocene analogue of **5a** + **5b,** could be prepared by Schiff base condensation of salicylaldehyde and aminoferrocene.[26] Deprotonation and in situ trapping with LDA/BF_3·Et_2O cleanly afforded its difluoroboronyl adduct **8** as a dark purple solid. The crystal structure of **8** is shown in Figure 5; selected bond lengths and angles are listed in Table 2.

UV−Vis Spectroscopy and Electrochemistry. The triferrocene compounds **5a** + **5b** display intense visible bands at λ_{max} = 370 nm (ϵ = 49 000 M^{-1} cm^{-1}) and 475 nm (ϵ = 15 600 M^{-1} cm^{-1}). The longer wavelength CT transition from the ferrocenyl fragment is similar to that (λ_{max} = 480 nm) of the monoferrocene analogue **7**, whereas the shorter wavelength transition is significantly red-shifted compared with that of **7** having vibronic progressions at λ_{max} = 310 and 338 nm (Figure 6). This feature arises from the extended

(35) Sobczyk, L.; Grabowski, S. J.; Krygowski, T. M. *Chem. Rev.* **2005**, *105*, 3513−3560.

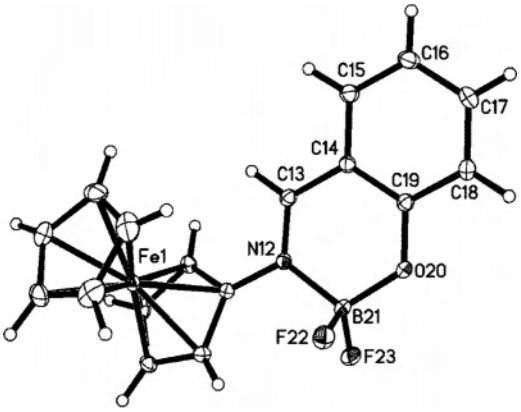

Figure 5. ORTEP diagram of **8** with thermal ellipsoids at 50% probability.

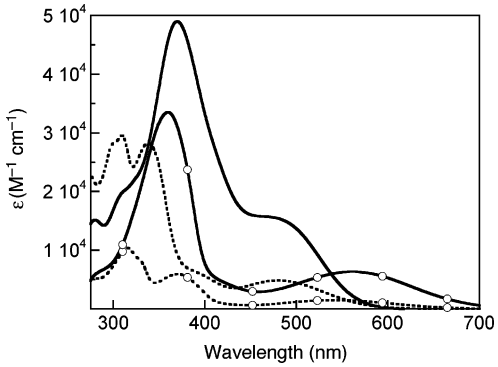

Figure 6. Electronic absorption spectra of **5a** + **5b** (—), **6** (— with circle), **7** (▪▪▪), and **8** (▪▪▪ with circle) in $CHCl_3$ at 298 K.

Table 3. Summary of Spectroscopic and Electrochemical Data for **5a** + **5b** and **6**−**8**

compd	λ_{max}, nm (ϵ, M^{-1} cm^{-1})	$E_{1/2}^{ox}$ (mV, vs Fc/Fc^+)	ΔE (mV)[a,b]
5a + **5b**	370 (49 000)	60	190
	475 (15 600)[c]		
6	360 (33 500)	210	112
	560 (6350)		
7	310 (29 600)	67	105
	338 (28 300)		
	480 (4860)		
8	315 (10 400)	193	90
	370 (5940)		
	545 (1510)		

[a] $\Delta E = |E_{pc} - E_{pi}|$. [b] Under similar conditions, the Cp_2Fe/Cp_2Fe^+ redox couple showed $\Delta E = 120$ mV. [c] Appeared as a shoulder at a peak position determined from derivative spectra.

[π,π]/[n,π]-conjugation of the tris(*N*-salicylideneamine) core.[24] For both **5a** + **5b** and **7**, weakening of the ligand field strength of the aminocyclopentadienyl group by coordination of the $\{BF_2\}^+$ unit apparently resulted in systematic red-shifts ($\Delta\lambda = 65-85$ nm) of the ferrocenyl transitions (Table 3). The impact of this electronic perturbation on the redox chemistry and possible electronic communications between adjacent redox-active sites were probed further by electrochemistry.

The cyclic voltammogram (CV) of **5a** + **5b** in CH_2Cl_2−CH_3CN (1:1, v/v)[36] displayed a broad ($\Delta E = 190$ mV) chemically reversible ($i_{pa}/i_{pc} \approx 1$) oxidation wave centered at $E_{1/2} \approx 60$ mV (Figures 7a and S2).[37] The overlapping components of this oxidation process were probed by differential pulse voltammetry (DPV). As shown in Figure 8, two partially resolved DPV peaks were observed for **5a** + **5b** at ca. +20 and +90 mV. Their combined integrated area was consistent with an overall 3-electron redox process when comparison was made against the signal from decamethylferrocene ($E_{1/2}^{ox} = -53$ mV) added as an internal reference (Figure 8a). This resolved feature, however, essentially merged to become a single DPV peak when measurements were made in DMF electrolytes (Figure S3).

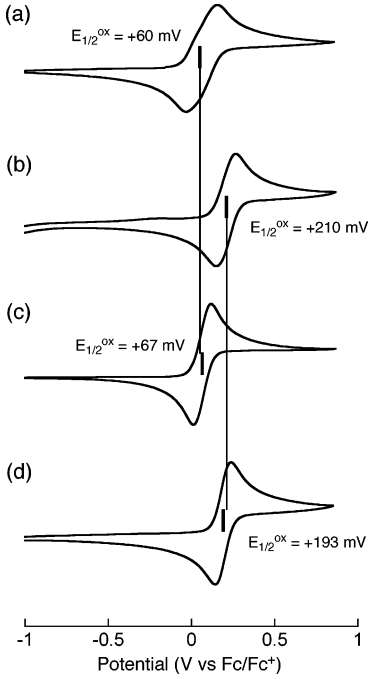

Figure 7. Cyclic voltammograms (scan rate = 150 mV) of (a) **5a** + **5b**, (b) **6**, (c) **7**, and (d) **8** in CH_2Cl_2−CH_3CN (1:1, v/v) at 25 °C with 0.1 M $(Bu_4N)(PF_6)$ as supporting electrolyte. Thick vertical lines indicate the position of $E_{1/2}^{ox}$ along the *x*-axis (= potential vs Fc/Fc^+). Thin vertical lines were added to aid direct comparison of this parameter between **5a** + **5b** and **7**, and between **6** and **8**, respectively.

In contrast to this complicated behavior of **5a** + **5b**, the electrochemistry of the corresponding tris(difluoroboronyl) adduct **6** showed a simple 3-electron redox process at $E_{1/2} = 210$ mV (Figures 7b and 8b). The systematic anodic shifts of $E_{1/2}$ upon coordination of $\{BF_2\}^+$ fragments, i.e., +150 mV for **5a** + **5b** → **6** and 126 mV for **7** → **8** (Figure 7), reflect the reduced donor ability of the nitrogen atoms bound to the Lewis acidic boron center. This observation is also consistent with the red shifts in the electronic transition of the ferrocenyl group originating from a decreased ligand field strength (vide supra).

Discussion

Design and Synthesis. Electronically conjugated C_3-symmetric systems have degenerate frontier orbitals, the

(36) In CH_2Cl_2, the cyclic voltammograms of **6** displayed a broad oxidation wave at +275 mV. Upon return sweep, however, a stripping-type reduction wave was observed at +105 mV, making the determination of $E_{1/2}$ values less than straightforward. The reversibility of this redox process could be significantly improved by employing a CH_2Cl_2−CH_3CN (1:1, v/v) mixed solvent, in which all subsequent electrochemical studies were conducted for direct comparison.

(37) Unless noted otherwise all potentials have been referenced vs Cp_2Fe^+/Cp_2Fe.

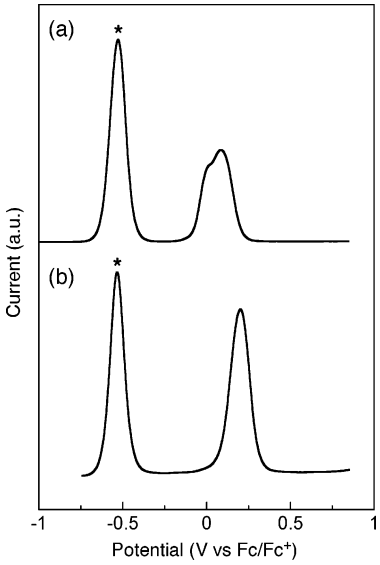

Figure 8. Differential pulse voltammograms (modulation time = 50 ms; modulation amplitude = 25 mV; pulse period = 250 ms; step potential = 5 mV) of (a) **5a** + **5b** and (b) **6** in $CH_2Cl_2-CH_3CN$ (1:1, v/v) at 25 °C with 0.1 M $(Bu_4N)(PF_6)$ as supporting electrolyte. The potential was externally referenced to the Cp_2Fe^+/Cp_2Fe redox couple. For each case, the signal from decamethylferrocene (3 equiv with respect to the triferrocene compound), added as an internal reference for peak integration, is marked with an asterisk (∗).

partial occupancy of which can potentially lead to materials displaying interesting electronic as well as magnetic properties. Research in such directions has produced numerous discotic planar conjugated systems.[38−41] Within this context, we have previously shown that the C_3-symmetric core of tris(*N*-salicylideneamine) can serve as a viable structural surrogate of 2,6,10-trisubstituted triphenylenes.[21,23,24,42,43] As shown in Figure 9, the three N−H···O═C resonance-assisted hydrogen-bonding (RAHB)[35,44,45] networks extended from the central six-membered ring of tris(*N*-salicylideneamine) (**F**) faithfully trace the shape of triphenylene (**E**)[46] and enforce planar rigidity. The root-mean-square (rms) deviation of the fitted atom pairs was 0.155 Å when comparisons were made

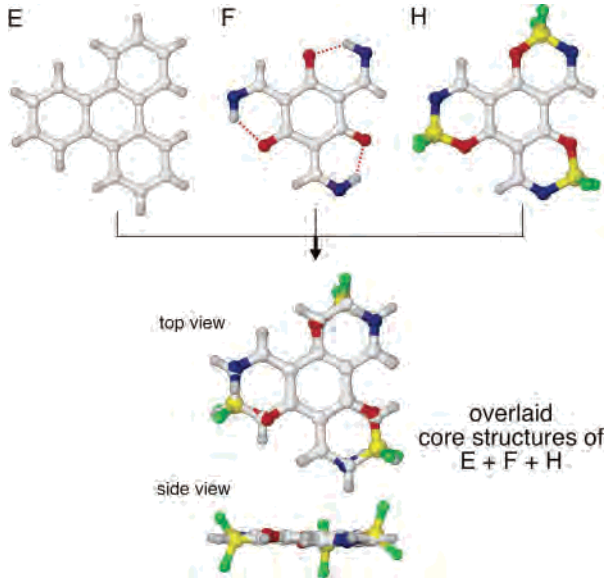

Figure 9. Structural comparison of the molecular core of triphenylene (**E**), tris(*N*-salicylideneamine) (**F**), and the tris(difluoroboronyl) complex of **F** (**H**). Shown below are overlaid core structures of **E**, **F**, and **H** and the side view in capped-stick models. The X-ray coordinates of **E** were obtained from CSD file TRIPHE12,[46] **F** from 2,4,6-tris(2,6-dimesitylphenylaminomethylene)-cyclohexane-1,3,5-trione,[23] and **H** from compound **6** and fitted by a least-squares minimization procedure using the crystallographic model manipulation program XP from the SHELXTL suite.[30] N is blue, O is red, B is yellow, and F is green.

Scheme 2

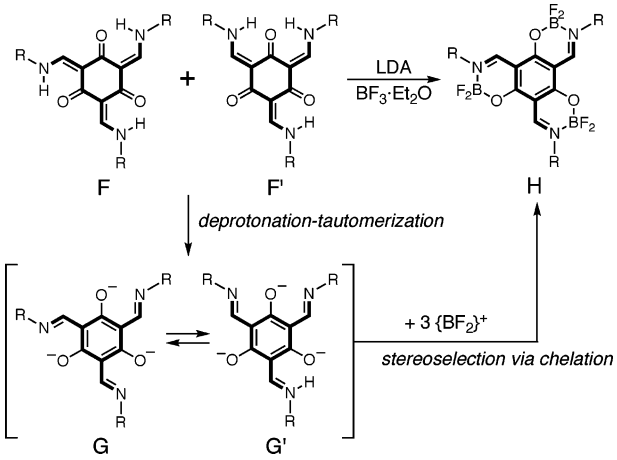

for the non-hydrogen atoms. In addition to this structural similarity, the highly convergent and modular [3 + 1] Schiff base condensation route allows for simplicity in the synthetic design and multiplicity in the selection of peripheral functional groups, thus facilitating structural modifications to explore possible through-bond electronic coupling interactions.

Despite these attractive features, however, the synthetic utility of tris(*N*-salicylideneamine)s has been significantly compromised by the coexistence of **F** and its geometric isomer **F′** (Scheme 2). As shown in Scheme 2, restricted rotations about the enamine C−C double bonds relate enthalpically favored **F** and entropically favored **F′**, which are typically inseparable in preparatory scales.[21,22] This synthetic challenge was previously met with the use of bulky aromatic groups[23] or with the installation of peripheral

(38) Müllen, K., Wegner, G., Eds. *Electronic Materials: The Oligomer Approach*; Wiley-VCH: New York, 1998.
(39) Watson, M. D.; Fechtenkötter, A.; Müllen, K. *Chem. Rev.* **2001**, *101*, 1267−1300.
(40) Bushey, M. L.; Nguyen, T.-Q.; Zhang, W.; Horoszewski, D.; Nuckolls, C. *Angew. Chem., Int. Ed.* **2004**, *43*, 5446−5453.
(41) *Chem. Rev.* **2005**, *105*, 3433−3947, thematic issue on "delocalization − pi and sigma".
(42) Pérez, D.; Guitián, E. *Chem. Soc. Rev.* **2004**, *33*, 274−283.
(43) For recent examples of heteroatom-containing structural mimics of triphenylenes, see the following: (a) Arikainen, E. O.; Boden, N.; Bushby, R. J.; Lozman, O. R.; Vinter, J. G.; Wood, A. *Angew. Chem., Int. Ed.* **2000**, *39*, 2333−2336. (b) Gearba, R. I.; Lehmann, M.; Levin, J.; Ivanov, D. A.; Koch, M. H. J.; Barberá, J.; Debije, M. G.; Piris, J.; Geerts, Y. H. *Adv. Mater.* **2003**, *15*, 1614−1618. (c) Ishi-i, T.; Murakami, K.-i.; Imai, Y.; Mataka, S. *Org. Lett.* **2005**, *7*, 3175−3178. (d) Jaska, C. A.; Emslie, D. J. H.; Bosdet, M. J. D.; Piers, W. E.; Sorensen, T. S.; Parvez, M. *J. Am. Chem. Soc.* **2006**, *128*, 10885−10896.
(44) (a) Gilli, G.; Bellucci, F.; Ferretti, V.; Bertolasi, V. *J. Am. Chem. Soc.* **1989**, *111*, 1023−1028. (b) Bertolasi, V.; Gilli, P.; Ferretti, V.; Gilli, G. *J. Am. Chem. Soc.* **1991**, *113*, 4917−4925. (c) Gilli, P.; Bertolasi, V.; Ferretti, V.; Gilli, G. *J. Am. Chem. Soc.* **2000**, *122*, 10405−10417.
(45) Chin, J.; Kim, D. C.; Kim, H.-J.; Panosyan, F. B.; Kim, K. M. *Org. Lett.* **2004**, *6*, 2591−2593.
(46) Collings, J. C.; Roscoe, K. P.; Thomas, R. L.; Batsanov, A. S.; Stimson, L. M.; Howard, J. A. K.; Marder, T. B. *New J. Chem.* **2001**, *25*, 1410−1417.

hydrogen-bonding networks,[24] which exclusively afforded the C_3-symmetric isomer **F**. Alternatively, a mixture of **F** and **F′** could be subjected to chemical transformations that can selectively furnish a single product. The latter approach can overcome the limited substrate scope associated with the former, as we have recently demonstrated by constructing a series of stackable *pseudo*-triphenylenes which display enhanced fluorescence efficiency as solution aggregates.[21]

As shown in Scheme 2, this *chelation-driven stereoselection* strategy takes advantage of deprotonation and subsequent tautomerization, which essentially converts the enamine C−C double bonds in **F** and **F′** to the freely rotating C−C single bonds in the enolate−imine intermediates **G** and **G′**. After being trapped with 3 equiv of $\{BF_2\}^+$, generated in situ from the reaction between $BF_3{\cdot}Et_2O$ and *n*-BuLi, the C_3-symmetric adduct **H** was obtained as the only product. The quantitative (>99%) and exclusive formation of **6** from an essentially equimolar mixture of **5a** and **5b** strongly supports the mechanism depicted in Scheme 2. Related $\{BX_2\}^+$ (X = F, Cl, or Br) complexes of mononucleating[47] as well as dinucleating[48] *N*-substituted Schiff base ligands[49] have previously been characterized.

As shown in Figure 9, the ring-fused core of **F** is geometrically analogous to **E**, with a rms deviation of 0.128 Å for all non-hydrogen atoms that were fitted. Related 1,3,5-trihydroxybenzene-based multinucleating ligands $\mathbf{L_1}^{3-}$, $\mathbf{L_2}^{6-}$, and $\mathbf{L_3}^{3-}$ support tricopper(II),[50,51] trinickel(II),[52,53] or dodecacopper(II)[54] complexes. The planar conjugated core of these ligand mediates ferromagnetic interactions between the metal centers[50,51] or electronic communication among nonproximiate π-systems at the periphery.[52,53] Intriguingly, the ^{1}H NMR spectra of the protonated free ligand $H_6\mathbf{L_2}$ (R = H; R′ = H) displayed complicated splitting patterns at room temperature, which was ascribed to the hindered rotation of the enol−imine structure[52] rather than the possible keto−enamine tautomerism and the coexistence of *pseudo* C_3- and C_s-symmetric isomers.

Planar Conjugation and Electronic Coupling. Electron hopping between adjacent redox-active centers serves as a self-exchange charge conduction mechanism for electroactive materials.[6−9] Previous research on linearly conjugated diferrocenyl compounds has established important structural parameters and geometric requirements of the [π,π] and/or [d,π]-conjugated spacers for low-energy-barrier self-exchange reactions in molecular wires and their models.[2,3,55−57]

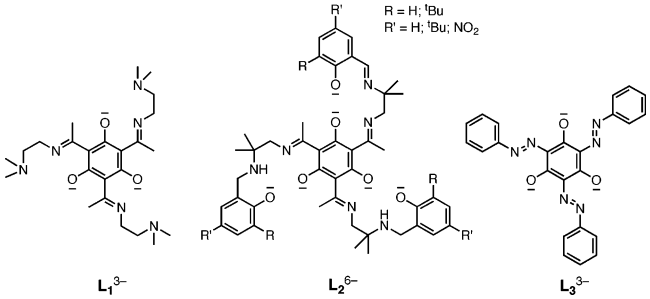

Despite the presence of a [π,π]/[n,π]-conjugated tris(*N*-salicylideneamine) core which significantly decreases the HOMO−LUMO gap and impacts the excited-state photophysics,[24] no significant electronic coupling was observed among the peripheral ferrocenyl units in **6**. Similar 3-electron process at single redox potential was also reported for **1** and **2**,[14d,16] indicating the instability of the transiently generated mixed-valent species supported by related C_3-symmetric platforms. Within this context, the overlapping redox waves measured for **5a** + **5b** in CH_2Cl_2−CH_3CN under CV and DPV conditions are noteworthy. An intuitive model for this phenomenon would invoke the contribution of the two isomers **5a** and **5b**, each with distinctive $E_{1/2}$ value, to the overall redox process observed. This scenario requires that the three ferrocenyl groups in each isomer undergo simultaneous one-electron oxidations at a single potential but this "apparent" $E_{1/2}{}^{ox}$ value is sufficiently sensitive to the core isomerism so that two separate oxidation waves are observed. This interpretation, however, is less consistent with the observation of a single DPV wave in DMF, especially considering that the ^{1}H NMR spectra of this material in DMF-d_7 revealed the coexistence of equimolar amounts of **5a** and **5b**. It is unlikely that this isomeric mixture would convert exclusively to a single species under the electrochemical conditions to provide a single redox wave. Alternatively, one could consider electronic communication through the hydrogen-bonded tris(*N*-salicylideneamine) core of **5a** + **5b**, which would result in stepwise oxidation of the peripheral ferrocenyl groups at distinctive $E_{1/2}$ values. The markedly different oxidation behavior of **5a** + **5b** in DMF implicates potential involvement of hydrogen-bonding interactions in such electronic coupling,[57,58] the disruption of which as a result of interaction with DMF could lead to disappearance of the stepwise oxidation processes and appearance of a single redox wave. The definitive answer to this question, however, awaits synthetic access to triferrocene derivatives having no stereochemical ambiguity associated with the tris(*N*-salicylideneamine) core isomerism.

Collectively, the synthesis and characterization of **5a** + **5b** and **6** significantly expands the class of triferrocene

(47) Xia, M.; Ge, S.-Q.; Li, X.-S. *Acta Crystallogr.* **2006**, *E62*, o2625−o2626.
(48) (a) Keizer, T. S.; Pue, L. J. D.; Parkin, S.; Atwood, D. A. *J. Am. Chem. Soc.* **2002**, *124*, 1864−1865. (b) Keizer, T. S.; De Pue, L. J.; Parkin, S.; Atwood, D. A. *Can. J. Chem.* **2002**, *80*, 1463−1468. (c) Keizer, T. S.; De Pue, L. J.; Parkin, S.; Atwood, D. A. *J. Organomet. Chem.* **2003**, *666*, 103−109.
(49) Atwood, D. A.; Harvey, M. J. *Chem. Rev.* **2001**, *101*, 37−52.
(50) Glaser, T.; Gerenkamp, M.; Fröhlich, R. *Angew. Chem., Int. Ed.* **2002**, *41*, 3823−3825.
(51) Glaser, T.; Heidemeier, M.; Grimme, S.; Bill, E. *Inorg. Chem.* **2004**, *43*, 5192−5194.
(52) Glaser, T.; Heidemeier, M.; Lügger, T. *Dalton Trans.* **2003**, 2381−2383.
(53) Glaser, T.; Heidemeier, M.; Fröhlich, R.; Hildebrandt, P.; Bothe, E.; Bill, E. *Inorg. Chem.* **2005**, *44*, 5467−5482.
(54) Abrahams, B. F.; Egan, S. J.; Robson, R. *J. Am. Chem. Soc.* **121**, *121*, 3535−3536.
(55) Robertson, N.; McGowan, C. A. *Chem. Soc. Rev.* **2003**, *32*, 96−103.
(56) Ren, T. *Organometallics* **2005**, 24, 4854−4870 and references cited therein.
(57) Sun, H.; Steeb, J.; Kaifer, A. E. *J. Am. Chem. Soc.* **2006**, *128*, 2820−2821.
(58) Yang, J.; Seneviratne, D.; Arbatin, G.; Andersson, A. M.; Curtis, J. C. *J. Am. Chem. Soc.* **1997**, *119*, 5329−5336.

derivatives built on planar conjugated cores. Our high-yielding two-step synthetic protocols involving [3 + 1] condensation and chelation-driven stereoselection should be generally applicable to a diverse array of conformationally rigid structural platforms, affording novel basis to correlate geometric and electronic factors responsible for electronic communication. Such efforts are currently underway in our laboratory.

Acknowledgment. This work was supported by Indiana University, the National Science Foundation (Grant CAREER CHE 0547251), and the American Chemical Society Petroleum Research Fund (Grant 42791-G3). We thank Mr. Xuan Jiang for assistance in acquiring the UV−vis spectra.

Supporting Information Available: Spectroscopic and electrochemical characterization of **5a** + **5b** (Figures S1−S3) and crystallographic data (CIF). This material is available free of charge via the Internet at http://pubs.acs.org.

IC062029V